Exposure and Health
https://doi.org/10.1007/s12403-023-00590-9

ORIGINAL PAPER

Quantifying the Health Risks of $PM_{2.5}$-Bound Heavy Metals for Rural Populations with Different Energy Use Types During the Heating Season

Wenju Wang[1] · Mingya Wang[1] · Mingshi Wang[1] · Xuechun Zhang[1] · Qiao Han[2,3] · Chun Chen[4,5] · Dan Liu[4,5] · Qinqing Xiong[1] · Chunhui Zhang[1]

Received: 16 January 2023 / Revised: 17 May 2023 / Accepted: 14 July 2023

Abstract

Premature deaths in China due to exposure to $PM_{2.5}$-bound heavy metals (HMs) are notably more prevalent in rural areas than in urban ones. In suburban rural areas, electricity and natural gas have emerged as the primary energy sources. However, in remote rural locations far from urban centers, coal and biomass are still commonly used for cooking and heating. This disparity in energy use can lead to variations in health risks among populations and may cause significant discrepancies between implemented policies and actual conditions. Winter $PM_{2.5}$ samples were collected from rural sites across the North China Plain. To identify the effects of air exposure on rural populations with different types of energy use, we employed probabilistic and source-specific risk assessment methods. Results showed that the average $PM_{2.5}$ mass was 10.08 and 10.91 times higher than the World Health Organization's recommended guideline (15 μg/m^3). This indicates a higher contamination burden in suburban rural areas. Children were found to be at higher risk of noncarcinogenic risks (NCR) but at a lower risk of carcinogenic risks (CR) compared to adults. Interestingly, the NCR and CR of HMs from coal and biomass combustion in remote rural areas were 2.68 and 2.47 times higher, respectively, than those in suburban rural areas. The widespread use of electricity and natural gas in suburban areas has decreased the health burden of HMs on residents when compared to the use of coal and biomass. Coal and biomass combustion was identified as the primary source of health risks in remote rural areas. In suburban rural areas, it is essential to reduce coal and biomass combustion, vehicle emissions, and industrial emissions. Our results provide valuable scientific insights for the prevention of air pollution throughout the rural energy transition process, not only in China but also in developing countries worldwide.

Keywords Air pollution · Rural energy use · Probabilistic health risk · Source-specific health risk

Introduction

Exposure to hazy weather pose a significant public health issue for global populations. This is due to the associated health hazards, reduced visibility, and slow dispersion time (Chen et al. 2021; Quan et al. 2014). Although they constitute approximately only 10% of $PM_{2.5}$ mass, particle-bound heavy metals (HMs) pose a significant threat. They are carcinogenic, non-degradable, and highly enriched (Lai et al. 2015; Xie et al. 2019). Pb (lead) exposure, in particular, can severely impact the development of children's cognitive abilities (Liu et al. 2018a). Other metals, such as Ni (nickel), Cr (chromium), Mn (manganese), and Co (cobalt), can infiltrate the human body and cause DNA damage, leading to impaired respiratory function (Chen et al. 2021; Feng et al. 2022a). HMs present in respirable particulate matter

✉ Mingya Wang
wangmy@hpu.edu.cn

Wenju Wang
719697076@qq.com

1 College of Resource and Environment, Henan Polytechnic University, Jiaozuo 454003, China

2 Institute of Geochemistry, Chinese Academy of Sciences, Guiyang 550081, China

3 University of Chinese Academy of Sciences, Beijing 100049, China

4 Henan Ecological Environment Monitoring and Safety Center, Zhengzhou 450046, China

5 Henan Key Laboratory for Environmental Monitoring Technology, Zhengzhou 450004, China

Published online: 27 September 2023

represent key pollutants threatening human health (Hus et al. 2021; Wang et al. 2019b, 2022).

The quantification of health risks to populations exposed to air pollution, which is the foundation for research to assess the local public health burden accurately, is already underway in many cities and regions (Faraji Ghasemi et al. 2020; Peng et al. 2017). Currently, health risk studies of $PM_{2.5}$-bound HMs depend excessively on point estimates with deterministic parameters; meanwhile, the variability of exposure factors between individuals, such as body weight and duration of exposure, are ignored; this approach may severely underestimate or overestimate risk values (Huang et al. 2021). However, probabilistic risk assessment based on Monte Carlo simulation (MCS) ensures the accuracy of risk calculations by integrating the proportion of risk thresholds that are exceeded and those that are not, and its reliability was confirmed in the previous studies (Widziewicz and Loska 2016). The toxicity of atmospheric HMs emitted by different sources varies (Bell et al. 2014). Source apportionment models are a proven technique for accurately identifying the sources of environmental pollutants and have been widely used in source analysis studies of atmospheric, water, and soil pollutants (Ma et al. 2018; Xie et al. 2020; Hus et al. 2021). Source-specific risk assessment based on source apportionment models has received increasing attention recently (Liu et al. 2018a; Yan et al. 2022). A reasonable assessment of the health risk caused by $PM_{2.5}$-bound HMs from multiple perspectives is still an open topic (Men et al. 2021; Heidari et al. 2021). In the present study, health risk assessment based on probabilistic and source-specific risks was explored to provide more reliable evidence for quantifying regional population health burden and controlling pollution sources.

$PM_{2.5}$-bound HMs enter the body through various pathways that increase the incidence of cardiovascular and respiratory disease and even cause premature death by inducing oxidative stress and systemic inflammation (Guo et al. 2021; Jimenez et al. 2009). The all-cause mortality rate (deaths from all causes as a proportion of the total population) among Chinese residents was about seven per 1000 in 2018; deaths due to cardiovascular and respiratory systems accounted for 57.9% of the all-cause deaths in rural areas, compared with 54.6% in urban areas (National Bureau of Statistics of China, http://www.stats.gov.cn/; China National Center for Cardiovascular Disease, https://www.nccd.org.cn/). The health of rural residents may be more sensitive to air pollution than that of urban populations. Previous studies have shown that agricultural activities and using biomass energy and coal in rural areas lead to more haze events (Du et al. 2018; Hu et al. 2019). Although rural China is promoting energy transition, it is still quite limited in many rural areas (Liu and Ren 2020; Zhao et al. 2020). Outdoor exposure of the population is exacerbated by the poor planning of rural buildings and the occupational characteristics of farmers who regularly engage in outdoor activities (Liu and Ren 2020; Liu et al. 2016). A report contended that rural residents are more sensitive to air pollution than urban residents by using a distributed lag nonlinear model, and $PM_{2.5}$ is an essential factor that causes premature mortality in rural areas (Zhao et al. 2021). The public health burden on Chinese rural residents has long been neglected. Approximately 40% of the Chinese population faces serious health threats from air pollution while not receiving widespread social attention.

Suburban rural areas located on the outskirts of cities are gradually being classified within the scope of centralized urban heating because of the advancement of China's urban infrastructure; the ban on coal and biomass use is more stringent than that in remote rural areas, and electricity and natural gas become the only forms of energy utilization in suburban rural areas (Wang et al. 2021a). A survey in Tangshan, China, has demonstrated significant differences in the characteristics and sources of outdoor $PM_{2.5}$ in coal-fired and centrally heated areas (Wang et al. 2021a), and different types of energy utilization may cause variations in population health risks in rural areas (Feng et al. 2021). However, the characteristics of air pollution in rural areas are not fully recognized due to the difficulty in obtaining information on haze pollution and the decentralized distribution characteristics. Studies on the health risks of rural populations under $PM_{2.5}$ exposure are scarce, and research on different rural types has never been conducted. To fill this gap, health risks from $PM_{2.5}$-bound HMs to rural populations of different energy use types were investigated based on probabilistic and source-specific risk assessment models. This work may contribute to a comprehensive understanding of the effect of air pollution on the target population's public health burden. Now insights into air pollution control in the rural energy transition process in developing countries around the world are also provided.

Materials and Methods

Sampling Sites

The North China Plain (NCP), which is the second largest plain in China, is located at latitude 32°–40° North and longitude 114°–121° East and has a temperate monsoon climate. NCP is an area in China with a high population, rural agglomeration, and well-developed agriculture; it is one of the most polluted areas in China in terms of haze (Jin et al. 2020; Wang et al. 2015). Two rural sites located in the western portion of the NCP, Qizhuang Village (QZV; 36° 11′ 15″ N, 114° 23′ 51″) and Liuji Village (LSV; 36° 11′ 15″ N, 114° 22′ 41″), Anyang were considered in this study, as shown in Fig. 1. Anyang is a typical heavy industrial city, and its

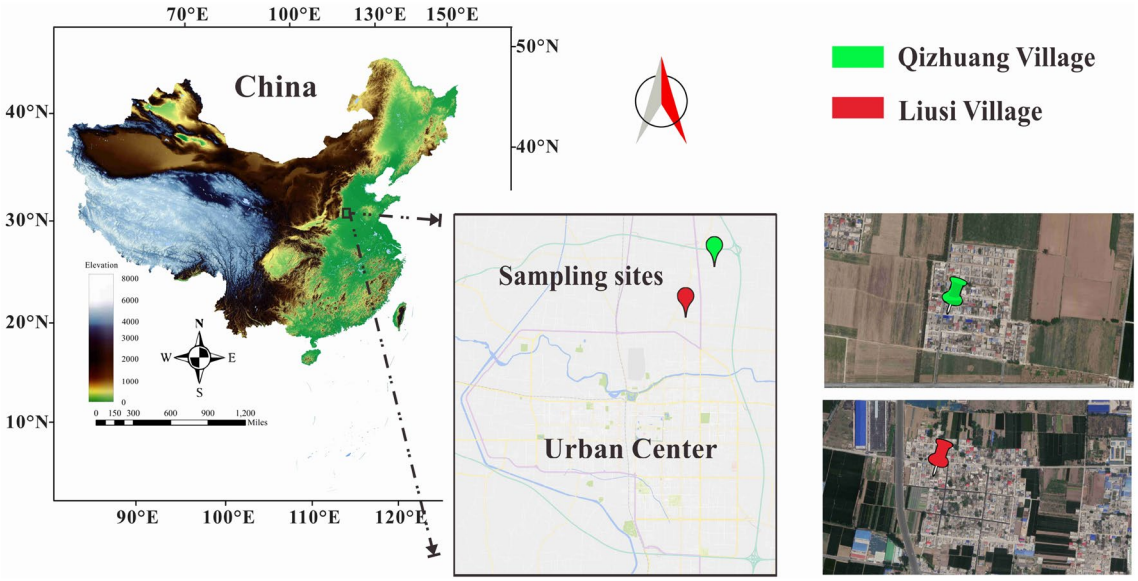

Fig. 1 Location of sampling sites

leading industrial products are steel product, steel, pig iron, and coke. $PM_{2.5}$ filter samples were simultaneously collected at two rural sites during the heating season from November 24 to December 3, 2020. An atmospheric sampler was set up on the roof of a specific residential building (about 5 m above the ground) at each rural site. QZV, which is far from the urban center and surrounded by much farmland, is a remote rural site. After our actual investigation, industrial agglomeration was observed about 4 km to the west and east of QZV. The Beijing–Hong Kong–Macao Expressway was about 1.6 km east of the sampling site. The nearby factories and roads might contribute to air pollution. During the sampling period, residential chimneys frequently produced smoke from coal combustion because the sampling site was outside the centralized city heating range. This situation is a widespread phenomenon in remote rural areas of China far from urban centers. Although the former bulk coal was primarily replaced by clean coal at the government's request, coal combustion emissions still require attention. QZV has similar contamination sources to its surrounding villages and reflects the air pollution characterization in remote rural areas in China. According to the Chinese urbanization process, factories and enterprises in the former urban areas have been relocated to the suburbs (Liu 2013). LSV is a suburban rural site with many factories, including steel smelting, thermal power generation and mechanical engineering, within 1 km of the site, and large steel smelters located approximately 6 km to the west and 9 km to the northwest. In addition, the urban roads around LSV were denser than those around QZV. The local government department vigorously promoted the measure of "zero loose coal and natural gas coverage in villages" during the sampling period. LSV is located in a centralized heating zone of the city, where the use of coal and biomass for heating in winter has completely disappeared. The air pollution characteristics of LSV are representative of the rural suburbs of China.

$PM_{2.5}$ Sampling and HM Analysis

The 12 h continuous $PM_{2.5}$ samples (from 9:00 to 21:00) were collected on Teflon filters using an atmospheric sampler of medium flow rate (KDB-120B; at a flow rate of 0.96 ± 0.04 L/min). Blank filters were also collected to eliminate the effect of atmospheric background values of crustal elements, such as Ca, Fe, and Al (Feng et al. 2022b; Xu et al. 2016). The volume of air passing through the filter for each sample was recorded at the end of sampling, and all filter samples were equilibrated in a clean room at a constant temperature and humidity (22 ± 2 °C, 40 ± 5%) for 48 h. The filters were weighed with an electronic microbalance before/after sampling (MS105DU, Mettler-Toledo, Switzerland). A total of 38 filter samples were stored and sealed at − 4 °C until chemical analysis.

Quarter filter samples were chopped with ceramic scissors and placed in Teflon digestion tubes with 4 mL 60% nitric acid, 2 mL 40% hydrofluoric acid, and 0.5 mL 30% hydrogen peroxide. The metal elements were extracted in a microwave digestion system (Multiwave PRO, Anton Paar, Austria) under a specific temperature program. The digestion solution was evaporated to 1−2 mL on an electric hot plate heated to 120 °C for about 5 h. The extract was diluted to 20 mL by adding 5% HNO_3 after cooling, and the solution was passed through pinhole filters of 0.45 μm. Nine HMs (Co, Ni, Mn, Pb, Cr, Zn, As, V, and Cu) and six conventional

metal elements (K, Mg, Ca, Na, Al, and Fe) were analyzed with an inductively coupled plasma optical emission spectrometer (PerkinElmer Optima 8000, USA).

Quality Control in Analysis

The standard reference material (GBW-07401, National Research Centre for Certified Reference Materials, China) and blank filters were analyzed in the same way as the samples to achieve quality assurance and control. The analytical results for all samples were subtracted from the blank control to reduce the error caused by the background values. Average repeatability of less than 6% was obtained for 15 metal elements with recoveries that ranged from 89.5 to 109.2% (Table S1). The detection limits of K, Mg, Ca, Na, Al, Fe, Co, Ni, Mn, Pb, Cr, Zn, As, V, and Cu were 1.00, 0.04, 0.05, 0.5, 1.00, 0.10, 0.20, 0.50, 0.10, 1.00, 0.20, 0.20, 1.00, and 0.50 μg/L, respectively. If the element concentration is below the detection limit, then half the detection limit is used instead.

Evaluation of $PM_{2.5}$-Bound HM Contamination

The pollution risk of $PM_{2.5}$-bound HMs was quantified by using the ecological risk index (ERI) proposed by Swedish geochemist Hakanson in 1980 (Hakanson 1980). The method is frequently adapted to HM pollution assessment and ecological risk evaluation in atmospheric particulate matter (Zhang et al. 2021). The ERI was calculated as follows:

$$ERI = \sum_{i}^{m} E_{\mathrm{r}}^{i} = \sum_{i}^{m} T_{\mathrm{r}}^{i} \times C_{f}^{i} = \sum_{i}^{m} T_{\mathrm{r}}^{i} \times \frac{C_{sample}^{i}}{C_{crust}^{i}}, \quad (1)$$

where E_{r}^{i} is the potential ecological risk coefficient of the i_{th} HM, T_{r}^{i} is the biotoxicity response coefficient of the i_{th} metal, C_{f}^{i} is the contamination factor, C_{sample}^{i} is the content of the i_{th} metal in the sample, and C_{crust}^{i} is the soil background value of the i_{th} HM. In this study, the E_{r}^{i} values of nine HMs were estimated. The biotoxicity response factors of Co, Ni, Mn, Pb, Cr, Zn, As, V, and Cu were chosen as 5, 5, 1, 5, 2, 1, 10, 2, and 5, respectively, according to the previous studies (Zhang et al. 2021; Zhi et al. 2021; Liu et al. 2018b). The ERI ranking of HMs in $PM_{2.5}$ is shown in Table S1.

Source Identification Method

Positive matrix factorization (PMF), which was proposed by Paatero and Tapper (1994), is a useful tool for determining the source and contribution of $PM_{2.5}$-bound HMs. PMF does not require measurements of the source component spectrum and has nonnegative species contribution in the decomposition matrix compared with other source apportionment models (Paatero and Tapper 1994; Hassan et al. 2021). The principle of the PMF model can be obtained from previous studies (Xie et al. 2020; Amato and Hopke 2012).

In this study, the concentrations of 15 metal elements (K, Mg, Ca, Na, Al, Fe, Co, Ni, Mn, Pb, Cr, Zn, As, V, and Cu) and $PM_{2.5}$ were inputted into the model to calculate the composition spectrum and contribution of each factor. The optimal solution of the model was tested between two and seven factors according to the $Q_{\mathrm{robust}}/Q_{\mathrm{ture}}$ value. The result showed that the model was most reliable when the number of factors was four.

The uncertainty test of the PMF model is essential due to the limitation of the sample size, data variability, model structure instability, and parameter sensitivity. Displacement (DISP) and BootStrap (BS) methods recommended by Paatero et al. (2014) were applied to obtain error estimates for source assignment. Additional details of these approaches to uncertainty analysis were presented in previous studies (Men et al. 2019; Paatero et al. 2014).

Probabilistic Health Risk Assessment

The probabilistic health risk assessment is predicated on the health risk assessment model provided by the US EPA (2011), with thousands of samples obtained using MCS and the results presented in a statistical manner (Xie et al. 2017). Airborne HMs pose health risks to humans in three ways, namely, direct inhalation by the respiratory system, ingestion of food to which HMs are attached, and dermal absorption of HMs deposited on the skin surface (Han et al. 2021a; Wang et al. 2019a; Zhang et al. 2018). The average daily exposure (ADD) for the three pathways was calculated by using the following equation:

$$\mathrm{ADD}_{\mathrm{inhalation}} = \frac{C \times \mathrm{Inh}R \times \mathrm{EF} \times \mathrm{ED}}{\mathrm{PEF} \times \mathrm{BW} \times \mathrm{AT}}, \quad (2)$$

$$\mathrm{ADD}_{\mathrm{ingestion}} = \frac{C \times \mathrm{EF} \times \mathrm{Ing}R \times \mathrm{ED}}{\mathrm{BW} \times \mathrm{AT}} \times \mathrm{CF}, \quad (3)$$

$$\mathrm{ADD}_{\mathrm{dermal}} = \frac{C \times \mathrm{SA} \times \mathrm{SL} \times \mathrm{ABS} \times \mathrm{EF} \times \mathrm{ED}}{\mathrm{BW} \times \mathrm{AT}} \times \mathrm{CF}, \quad (4)$$

where C is the measured concentration of HM (mg kg^{-1}). The detailed interpretations and reference values for other parameters are presented in Table S2.

Noncarcinogenic risk (NCR) and carcinogenic risk (CR) characterization is the final step in quantifying exposure to $PM_{2.5}$-bound HMs. The NCR of a single metal is expressed as a hazard quotient (HQ). The hazard index (HI), which is the sum of the HQ of all HMs, is used to assess the comprehensive NCR of exposure to multiple pollutants, as shown in the following formula:

$$HQ = \frac{ADD}{RfD}, \tag{5}$$

$$HI = \sum_{i=1}^{k} HQ_i = HQ_{inhalation} + HQ_{ingestion} + HQ_{dermal}, \tag{6}$$

where *RfD* is the reference toxicity threshold of HMs in diffident pathways. If HQ or HI ≥ 1, then the exposed population is at risk of severe NCR (Zhang et al. 2018), and the corresponding level of risk substantially increases with the improvement in HQ and HI.

The CR is the potential risk value of developing various cancers in humans by different exposure routes, and the total CR (TCR) is the sum of the CR of all $PM_{2.5}$-bound HMs. Both factors are calculated as follows:

$$CR = ADD \times SF, \tag{7}$$

$$TCR = \sum_{i=1}^{k} ADD_i \times SF_i, \tag{8}$$

where *SF* is the cancer slope factor of each HM under three exposure pathways. CR or TCR less than 10^{-6} is considered safe, while values greater than 10^{-4} indicate an unacceptable CR (Behrooz et al. 2021).

According to the International Agency for Research on Cancer (IARC 2016), Cr (VI), Ni, Pb, Co, and As were confirmed as carcinogenic HMs. Mn, Zn, V, and Cu were used only to calculate the NCR of the exposed population. The concentration of Cr (VI) was calculated using 1/7 of the Cr concentrations in this study (Massey et al. 2013).

The MCS was performed by loading Oracle Crystal Ball v11.1.24 (Oracle, USA) in Microsoft Excel. The various parameters in the traditional health risk assessment were separately imported according to the type of statistical distribution to which they belong (Table S4). The distribution type for each metal was fitted with a time series of measured concentrations using Crystal Ball software. In the end, the health risks of different populations were outputted after 10,000 MCSs.

Results and Discussion

Overview of the $PM_{2.5}$ Mass

The temporal variation of the $PM_{2.5}$ average concentrations at two rural sites from November 24 to December 3, 2020 is presented in Fig. 2. During the heating season, the $PM_{2.5}$ masses in the QZV and LSV were 39.90–266.21, and 85.25–282.43 μg m^{-3}, respectively, with mean values of 151.19 ± 64.61 and 163.72 ± 61.01 μg m^{-3}, respectively. The mean concentrations of $PM_{2.5}$ at both sites were much higher than those in some urban centers in China, such as Luoyang (91.1 μg m^{-3}, 2019.10–2020.01) (Xu et al. 2022), Nanjing (113 μg m^{-3}, 2014.01–02) (Kong et al. 2015), and Shanghai (65.0 μg m^{-3}, 2015.11–12) (Huang et al. 2018). The degree of fine particulate matter contamination in rural areas, which receive less concern, far exceeds that in some urban areas in China. In Fig. 2, all $PM_{2.5}$ filter samples

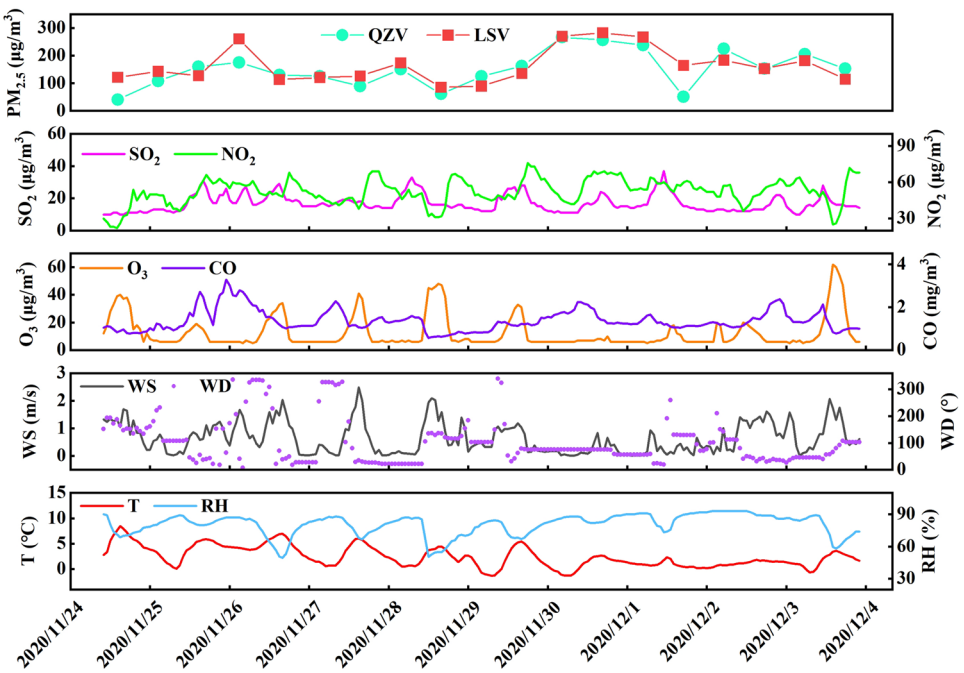

Fig. 2 Time series of the $PM_{2.5}$ mass and meteorological data during the sampling period. (WD, wind direction)

exceeded the 24 h $PM_{2.5}$ mass guideline recommended by the WHO (15 μg m^{-3}). Three samples from QZV blew the national ambient air quality standards by the Ministry of Ecology and Environment of the People's Republic of China (GB3095-2012) (daily average grade II, 75 μg m^{-3}) out of a total of 38 samples collected from two rural sites. The burden of air pollution was higher in suburban rural than in remote rural areas, which may be related to the proximity to urban centers and the presence of more potential pollution sources. LSV was surrounded by several factories, dense suburban roads, and the Chinese national road G107, and the high $PM_{2.5}$ levels might be associated with factory exhaust and vehicle emissions. Coal and biomass feedstock burning is the main form of winter heating in remote rural areas of northern China, while combustion for heating might be the leading cause of severe local haze events in QZV.

Multiple significant haze events were observed at both sampling sites in this study. In addition to the influence of anthropogenic activities such as coal combustion and industrial production, meteorological conditions were considered critical drivers for the rapid growth of $PM_{2.5}$. Hourly data of meteorological factors, including wind speed (WS), wind direction (WD), temperature (T), and relative humidity (RH), and gaseous pollutants such as SO_2, NO_2, CO, and O_3 were provided by Anyang Ecology and Environment Bureau. The average RH was 80.50% during the sampling period, and it reached 93% when the atmospheric visibility significantly decreased. The high RH provides appropriate requirements for the heterogeneous reaction of aerosols, which causes the production of numerous secondary pollutants such as sulfates. The mean WS during the sampling period was 0.64 m/s, and the frequent stationary weather sharply diminished the diffusion of the fine particulate matter. In the haze episode from November 29th 22:00 to December 1st at 10:00, the average RH and WS were 86.26% and 0.21 m/s, when the highest $PM_{2.5}$ mass concentrations peaked at 266.21 and 282.43 μg m^{-3}, respectively. Adverse meteorological conditions also played a dominant role in $PM_{2.5}$ accumulation. Severe haze occurred in LSV from 22:00 on November 25th to 10:00 on November 26th. The average WS at this time was 0.86 m/s, which was markedly higher than the average level. The proximity transport of pollutants emitted from nighttime production emissions in the surrounding factories could be a key contributor to the severe haze in LSV. By contrast, the decrease in $PM_{2.5}$ mass concentration was related to the reduction in pollutants from the surrounding factories and favorable atmospheric dispersion conditions.

Mass and Pollution Assessment of Metal Elements

The descriptive statistics of the 15 metal elements at two sites are shown in Table 1, and the average mass follows the sequence K > Ca > Fe > Al > Na > Mg > Zn > Pb > As > Co > Mn > Ni > Cr > Cu > V in QZV while Ca > K > Fe > Al > Na > Mg > Zn > Pb > Mn > As > Ni > Cu > Cr > V > Co in LSV during the heating season. Similar characteristics of HM contamination were observed in two rural sites. The mean Co, Pb, and As concentrations of QZV were significantly higher than those of LSV. Co, Pb, and As are released when fossil energy sources such as coal and oil are burned (Liu et al. 2019). The contribution of coal combustion emissions to atmospheric $PM_{2.5}$ around QZV was likely greater than that of LSV, which confirms that coal is still the primary energy in remote rural areas of China. Although several measures replacing coal with natural gas and electricity have

Table 1 Summary statistics of metal element concentrations in $PM_{2.5}$ (ng m^{-3})

Special	QZV				LSV			
	Mean	Median	SD	CV%	Mean	Median	SD	CV%
K	1583.99	1359.89	818.11	51.65	1259.56	1206.04	435.43	34.57
Mg	218.15	202.87	115.45	52.92	185.71	183.25	112.27	60.45
Ca	1419.27	1264.52	789.28	55.61	1423.96	1515.43	1066.11	74.87
Na	830.33	777.00	368.66	44.40	657.04	546.10	413.37	62.91
Al	836.99	604.81	636.22	76.06	951.19	797.06	744.50	78.27
Fe	865.08	821.88	411.58	47.58	957.09	797.23	451.21	47.14
Co	49.24	37.16	30.40	61.75	11.97	11.44	5.42	45.30
Ni	22.06	16.95	17.70	80.23	26.29	26.24	12.43	47.30
Mn	41.35	40.14	15.92	38.49	50.34	47.13	17.56	34.89
Pb	97.34	86.33	41.74	50.89	52.28	58.03	16.70	27.74
Cr	18.92	16.96	9.70	51.28	18.41	15.80	6.54	35.53
Zn	163.26	162.94	49.57	30.36	232.97	219.24	87.42	37.52
As	58.63	46.77	31.78	54.21	39.85	38.62	14.08	35.64
V	10.24	7.79	6.92	67.53	14.75	13.71	4.53	30.72
Cu	12.53	12.18	5.08	40.58	23.56	23.19	7.62	32.33

been implemented in many parts of China, the implementation in remote rural areas has been far less intensive than in suburban rural areas closer to urban centers.

The E_r^i values of the six HMs were calculated, as presented in Fig. 3 (unit converted from μg m^{-3} to mg kg^{-1}). The ecological risk caused by atmospheric $PM_{2.5}$-bound HMs was markedly stronger in QZV than in LSV despite the lower average daily $PM_{2.5}$ mass, and this result is related to the high-enrichment level of HMs in QZV. With regard to the mean value of all samples, the E_r^i values for Ni, Mn, Cr, Zn, and V were all below 40, which indicates that the five HMs pose a slight risk to the environment. The ecological risk of Co reached a heavy risk level in QZV, but it was negligible in LSV, which is inseparable from the high Co concentration in QZV. The remaining HMs, including Pb, As, and Cu, severely threatened the ecological environment. The ERI of As was much higher than that of the eight other toxic HMs at both sites. Notably, the highest average E_r^i value in QZV reached an extremely heavy risk level. Although the suburban rural area had a higher $PM_{2.5}$ pollution burden, it was typically less environmentally risky than remote rural. The rural air environment of the NCP showed significant HM contamination and potential ecological risks, which should be addressed, especially As, Pb, Cu, and Co.

Source Distribution of Metal Elements

Based on the PMF model (Fig. 4), four sources of $PM_{2.5}$ were identified for each sampling site, namely, coal and biomass combustion, industrial emissions, dust sources, and vehicle emissions.

In the QZV site, factor 1 has high Zn, Cu, Mn, and Pb emissions. Zn, Cu, Mn, and Pb can be released using motor vehicle lubricants and the wear of tires and brake pads (Kong et al. 2020; Han et al. 2020). Accordingly, factor 1 can be identified as vehicle emissions, and it accounted for 17.25%. By the end of 2020, the number of motor vehicles in Anyang has reached 1,042,600 (AMBS 2021). Increasing motor vehicle ownership means that air pollution from vehicle emissions is not negligible, even in rural areas. Factor 2 was weighted by Ni, Cr, V, and Cu. In 2020, the output of steel products and steel in Anyang reached 18,106,100 and 16,441,900 tons, respectively (AMBS 2021). Metals, such as Ni, Cr, V, and Mn, are frequently added during the steelmaking process to achieve the best performance from the steel product (Liu et al. 2018a). Factor 2 can be considered an industrial emission source, and it accounted for 19.37%. Factor 3 has high Co, K, Pb, and As emissions and was treated as a coal and biomass combustion source, and it accounted for 36.51% (Fig. S1). Previous studies showed that Co and Pb were emitted during the combustion of fossil fuels such as coal (Simoneit et al. 1999). As is mainly from coal combustion (Chen et al. 2021). The field investigation was conducted during the heating season when coal burning for heating is a common occurrence. K is the signature species of biomass burning (Simoneit et al. 1999; Begum et al. 2004). The burning of agricultural waste still exists in rural northern China, despite that numerous bans on the burning of biomass materials such as straw were implemented. Factor 4 showed high loadings of Mg, Ca, Na, Al, and Fe, which can be designated as dust sources. This factor accounted for 26.87%. Al, Fe, Ca, and Na are crustal elements because

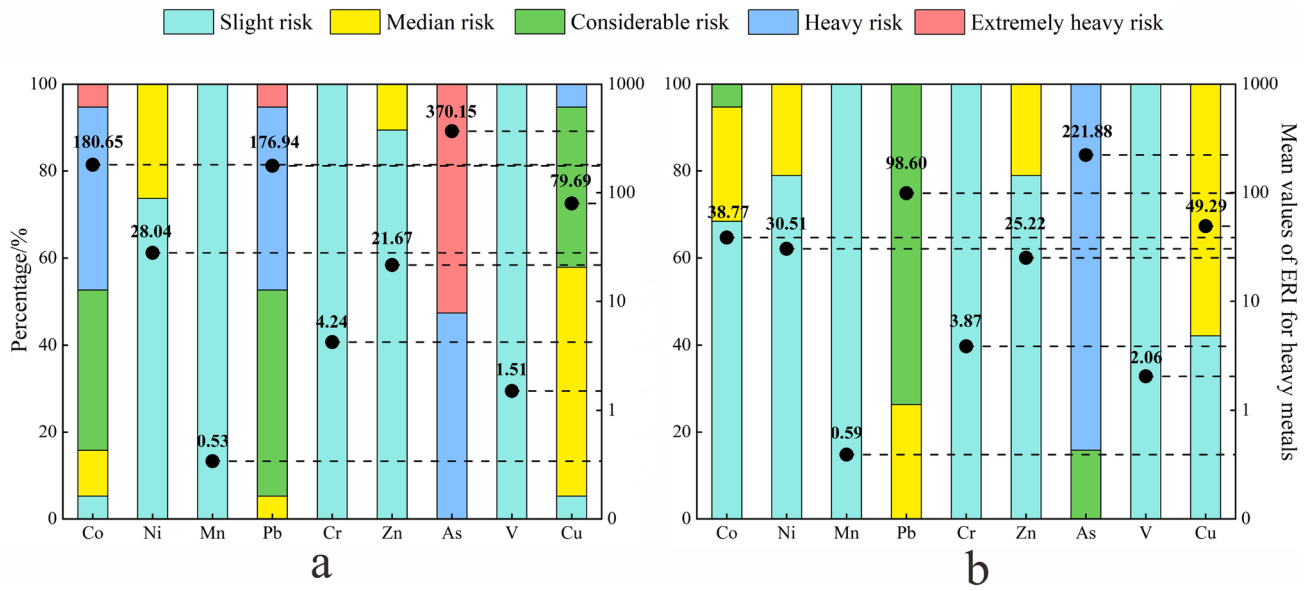

Fig. 3 Description of E_r^i in $PM_{2.5}$-bound HMs. (**a** QZV and **b** LSV, the black circle represents the mean value of E_r^i for heavy metals, and the black dashed line is the position of the mean value on the right coordinate axis)

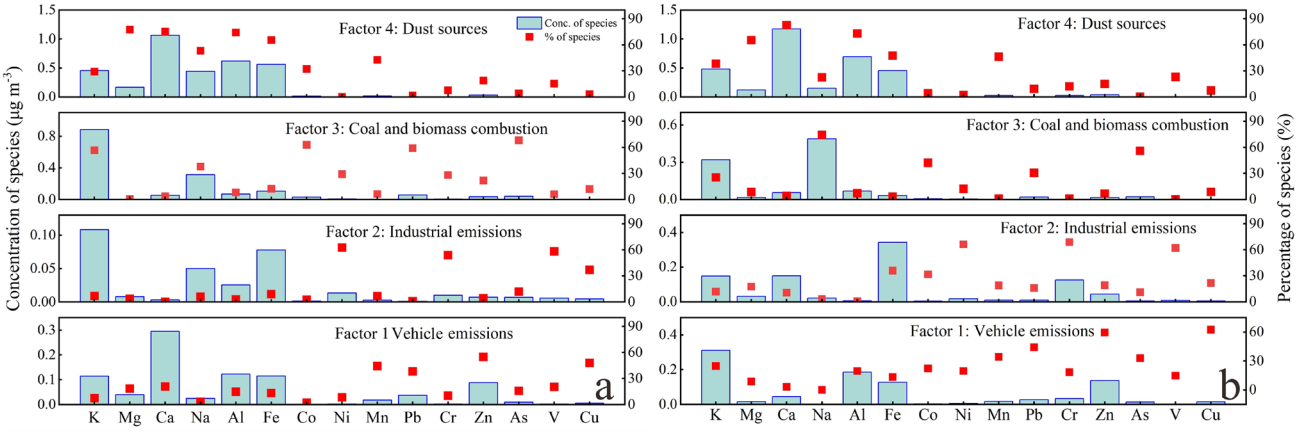

Fig. 4 $PM_{2.5}$ factor distribution characteristics and contribution based on the PMF model. (**a** QZV and **b** LSV)

they are the most abundant metallic elements in the Earth's crust. Mg is considered to be associated with construction dust (Zhao et al. 2019). In the LSV site, factor 1 has high Cu, Zn, and Pb emissions and can be considered a vehicle emission source, and it accounted for 27.92%. Factor 2 was mainly characterized by V, Ni, Fe, Cr, and Mn, which can be identified as industrial emissions. This factor accounted for 32.05%. High loadings of As, Na, Co, Pb, and K occurred in factor 3, and the burning of biomass feedstocks, such as corn stover releases Na (Simoneit et al. 1999; Begum et al. 2004). Accordingly, factor 3 was interpreted as coal and biomass combustion emissions, and it accounted for 32.11%. Factor 4 has high Mg, Ca, Al, and Fe emissions and can be identified as dust sources, and it accounted for 7.92%. During the heating period, coal and biomass combustion were the dominant sources of $PM_{2.5}$-bound HMs at both sites. The high percentage of this source in QZV was related to the lifestyle of remote rural residents who heat their homes by burning coal and biomass. However, coal and biomass combustion still contributed 32.11% despite that LSV is located in a centralized urban heating area. A large number of industrial enterprises with high consumption of coal and biomass existed around LSV, including thermal power generation and steel smelting. The high contribution of coal and biomass combustion may be related to the high consumption of energy sources such as coal and biomass in industrial production. In the present study, coal and biomass combustion was the main source of $PM_{2.5}$-bound HMs in remote and suburban rural areas, and the contribution of the former was apparently higher than that of the latter. The share of industrial and vehicle emissions in LSV was also much greater than that in QZV. This result can be explained by two reasons: one is that more factories are relocated from urban to suburban rural, and the other is that the road network is dense and the traffic load is relatively high in the suburban rural areas. For dust sources, the contribution in QZV was as high as 26.87%, which is much greater than the 7.92% in LSV. According to our investigation, a large amount of farmland around QZV had exposed soil and transported from the surface to the atmosphere by wind.

Uncertainty Analysis of the PMF Model

The DISP and BS methods were used to obtain the error estimate (EE) of source contribution obtained from PMF. DISP was typically determined as the first step in the selection solution. The frequency of factor swapping was inversely correlated with the feasibility of the model solution. The DISP swap results from the PMF model for both sites were less than 0.1% (Table S3), which indicates that the DISP swap performance was well, and the data inaccuracies were negligible. The DISP results were also acceptable because the percentage change in Q was less than 1% (Table S3), which is consistent with the results of previous research (Brown et al. 2015). In the BS test, the number of bootstrap runs was set to 100, the black size was 14, and the correlation R value was 0.6 (Paatero et al. 2014). The diagonal values of the mapping matrix from the BS to the base factors at the both sampling sites were between 83–98 and 85–97% (Table S3), respectively. This finding implies that the matching rate of BS factor was feasible. The uncertainty intervals of the estimation errors based on the BS and DISP methods are described in Table S6. The interval ratios, which are a crucial indicator of the error estimation results for different metal elements, were calculated by using the difference between uncertainty intervals divided by the 50th percentile or mean (Wang et al. 2021b). In Fig. S2, the trends of BS and DISP interval ratios were consistent, which shows that the uncertainty results of the two methods were in agreement. The metal elements with large interval ratios (near or equal to two) indicated significant uncertainty (Wang et al. 2021b). For instance, in the QZV site, K, Na, Co, Ni, and

Cr are present in factor 1, K, Mg, Ca, Al, Co, Pb, and Zn in factor 2, Mg, Ca, and V in factor 3, and Ni, Pb, As, and Cu in factor 4. In the LSV site, Ca, Al, Fe, Mn, Cr, Zn, and V are present in factor 1, Co, Ni, As, and Cu in factor 2, Na, Al, and As in factor 3, and Mg, Ca, and Na in factor 4. The interval ratio of BS was also greater than the interval ratio of DISP, which suggests that the random error accounted for a larger proportion of the uncertainty (Wu et al. 2020). Although certain uncertainties remained in the model, especially for species with a lower share, the four-factor solution of PMF model was deemed to be an optimal and reliable explanation in our study.

Probabilistic Risk Assessment of Rural Population

MCSs were used to derive probability NCR and CR for all residents (including children and adults) through three different routes in two rural areas. The descriptive statistics of the results are presented in Table 2.

The cumulative frequency plots of risk for the 10,000 simulation experiments are shown in Figs. 5 and 6. The health risks for all groups exposed to $PM_{2.5}$-bound HMs were consistent at rural sites in the NCP. The risk of outdoor $PM_{2.5}$ exposure for residents around QZV (HI of 4.38 for children, HI of 9.19E−01 for adults) was higher than that around LSV (HI of 2.70 for children, HI of 5.94E−01 for adults). Residents of remote rural areas were also more susceptible to the threat of NCR from haze exposure than those of rural suburban areas. The HI values in rural North China were much higher than those in Xinxiang urban area in the winter of 2014 (HI of 0.38 for children, HI of 0.21 for adults) (Feng et al. 2017), Shenzhen urban area in 2014–2020 (HI of 0.4 for children, HI of 0.3 for adults) (Yan et al. 2022), Kunming industrial area in 2013–2014 (HI of 0.26 for children, HI of 0.17 for adults) (Han et al. 2021b), and Beijing education area in 2016 (HI of 8.92E−01) (Liu et al. 2018a). The HI values were also lower than those in Xian and Nanchang urban areas (Li et al. 2021). The NCR in rural northern China was comparable to or even higher than those in some large cities, particularly in remote rural areas. The HI values were greater in children than in adults, which is consistent with the result of previous studies. Approximately 100% and 99.78% of children exceeded the risk threshold for HI, and children were more vulnerable to NCR than adults because of their habits of playing outdoor and licking contaminants attached to their hands (Zhang et al. 2021). The sensitivity of hemoglobin to HMs was also much higher than that of adults due to the fragile constitution of children (Sah et al. 2019). In this study, the trend of average HQ values for all population was As > Pb > Cr > Zn > V > Co > Mn > Cu > Ni in QZV, while the trend was As > Pb > Cr > V > Mn > Ni > Zn > Cu > Co in LSV. The high HQ of As was the dominant contributor to the increase in NCR. The HQ values of the remaining 6 HMs in children and adults were negligible except for As, Cr, and Pb.

According to the cumulative probability distribution of CR, the trend of average CR values for all population was As > Pb > Co > Cr > Ni in QZV. Meanwhile, the trend was As > Pb > Cr > Co > Ni in LSV. The 95% CIs of TCR were 1.61E−04–1.65E−04 and 9.74E−05–9.93E−05 for children and 2.33E−04–2.42E−04 and 1.39E−04–1.44E−04 for adults at the two rural sites, respectively, both of which significantly exceeded the acceptable risk threshold of 10^{-6}. Among the 10,000 statistical samples generated by MCSs, 74.19% and 82.31% of children and adults, respectively, showed a TCR exceeding 10^{-4} at QZV. Meanwhile, 38.18% and 57.29% of children and adults, respectively, showed such TCR at LSV. This result indicates that more than half of population was at risk of acute carcinogenic threats from $PM_{2.5}$-bound HMs. Residents in remote rural areas also faced much higher CR than suburban rural areas. Outdoor As and Pb exposure were the major drivers of high CR in all population. Notably, the mean CR values for As were near or even exceeded 10^{-4} at both sites, which suggests a remarkably severe cancer risk. The cancer risk of the remaining HMs, including Co, Ni, and Cr, was acceptable. In addition to Pb, the CR values were higher in adults than in children, which was related to the outdoor exposure time of the population due to occupation and lifestyle. Adults spend more time outside than children. More attention should be paid to rural areas, especially those far from urban centers, in alleviating haze pollution in China. Exposure of rural populations to airborne As and Pb through inhalation, ingestion, and dermal contact was the main cause of their high carcinogenic burden.

Quantification of Health Risks Based on Pollution Sources

PMF–HR, which is a combination of the source appointment model and health risk assessment, was applied to the source contribution of health risks in rural China based on MCSs of risk mean values. In Fig. 7, the health risk contribution rates from different sources demonstrated a high degree of consistency between adults and children. This finding is similar to that of the study in Shanghai urban park (Huang et al. 2021).

The source of the mean NCR for children and adults in QZV mainly includes coal and biomass combustion, vehicle emissions, and industrial emissions. Notably, coal and biomass combustion contributed approximately 63.62% and 59.68%, respectively. The high NCR values in remote rural areas were closely linked to the use of coal and biomass fuels for heating in winter, and HM emissions from coal and biomass combustion having NCR values for children and adults were 2.79 and 5.48E−01, respectively.

Table 2 Summary of NCR and CR based on Monte Carlo simulations

Sites	Risk parameters	Specials	Mean		Median		SD		95%CI	
			Children	Adult	Children	Adult	Children	Adult	Children	Adult
QZV	HQ	Co	5.41E−02	1.74E−02	4.45E−02	1.43E−02	3.87E−02	1.23E−02	(5.34E−02, 5.49E−02)	(1.72E−02, 1.77E−02)
		Ni	1.91E−02	3.77E−03	1.57E−02	2.90E−03	1.52E−02	3.34E−03	(1.88E−02, 1.94E−02)	(3.70E−03, 3.83E−03)
		Mn	2.33E−02	1.08E−02	1.95E−02	8.46E−03	1.55E−02	9.00E−03	(2.30E−02, 2.36E−02)	(1.07E−02, 1.10E−02)
		Pb	5.09E−01	1.15E−01	4.50E−01	2.60E−01	7.87E−02	7.87E−02	(5.04E−01, 5.14E−01)	(1.13E−01, 1.17E−01)
		Cr	1.63E−01	8.40E−02	1.30E−01	5.75E−02	1.31E−01	8.93E−02	(1.61E−01, 1.66E−01)	(8.22E−02, 8.57E−02)
		Zn	1.15E−02	2.42E−03	8.84E−03	1.79E−03	9.51E−03	2.23E−03	(1.13E−02, 1.17E−02)	(2.37E−03, 2.46E−03)
		As	3.51	6.48E−01	2.99	5.42E−01	1.99	4.15E−01	(3.48, 3.55)	(6.40E−01, 6.56E−01)
		V	6.90E−02	3.37E−02	5.77E−02	2.05E−02	4.46E−02	4.33E−02	(6.81E−02, 6.98E−02)	(3.28E−02, 3.45E−02)
		Cu	1.96E−02	3.83E−03	1.77E−02	3.36E−03	9.47E−03	2.26E−03	(1.94E−02, 1.98E−02)	(3.79E−03, 3.88E−03)
	HI	Total	4.38	9.19E−01	3.88	8.00E−01	2.23	5.42E−01	(4.34, 4.43)	(9.09E−01, 9.30E−01)
	CR	Co	4.41E−08	1.86E−07	3.67E−08	1.55E−07	3.06E−08	1.28E−07	(4.35E−08, 4.47E−08)	(1.83E−07, 1.88E−07)
		Ni	1.58E−09	6.64E−09	1.33E−09	5.61E−09	1.19E−09	5.01E−09	(1.55E−09, 1.60E−09)	(6.54E−09, 6.73E−09)
		Pb	1.20E−06	7.69E−07	1.07E−06	6.67E−07	6.05E−07	4.67E−07	(1.19E−06, 1.21E−06)	(7.59E−07, 7.78E−07)
		Cr	4.43E−08	6.43E−08	3.90E−08	5.72E−08	2.22E−08	3.17E−08	(4.38E−08, 4.47E−08)	(6.37E−08, 6.50E−08)
		As	1.62E−04	2.37E−04	1.33E−04	1.75E−04	1.10E−04	2.25E−04	(1.60E−04, 1.64E−04)	(2.32E−04, 2.41E−04)
	TCR	Total	1.63E−04	2.38E−04	1.35E−04	1.76E−04	1.10E−04	2.25E−04	(1.61E−04, 1.65E−04)	(2.33E−04, 2.42E−04)
LSV	HQ	Co	1.16E−02	3.74E−03	9.85E−03	3.18E−03	6.84E−03	2.19E−03	(1.15E−02, 1.17E−02)	(3.69E−03, 3.78E−03)
		Ni	2.04E−02	4.01E−03	1.92E−02	3.59E−03	9.66E−03	2.28E−03	(2.02E−02, 2.06E−02)	(3.96E−03, 4.05E−03)
		Mn	2.58E−02	1.19E−02	2.18E−02	9.39E−03	1.63E−02	9.16E−03	(2.54E−02, 2.61E−02)	(1.17E−02, 1.20E−02)
		Pb	2.85E−01	6.37E−02	2.68E−01	5.74E−02	1.01E−01	3.35E−03	(2.83E−01, 2.87E−01)	(6.31E−02, 6.44E−02)
		Cr	1.48E−01	7.63E−02	1.19E−01	5.16E−02	1.21E−01	8.34E−02	(1.46E−01, 1.51E−01)	(7.46E−02, 7.79E−02)
		Zn	1.30E−02	2.71E−03	1.11E−02	2.25E−03	7.48E−03	1.80E−03	(1.29E−02, 1.32E−02)	(2.67E−03, 2.74E−03)
		As	2.09	3.85E−01	1.96	3.53E−01	7.99	1.86E−01	(2.08, 2.11)	(3.82E−01, 3.89E−01)
		V	9.28E−02	4.56E−02	8.39E−02	2.98E−02	3.96E−02	5.38E−02	(9.20E−02, 9.36E−02)	(4.45E−02, 4.66E−02)
		Cu	1.20E−02	2.34E−03	1.13E−02	2.12E−03	4.94E−03	1.20E−03	(1.19E−02, 1.21E−02)	(2.31E−03, 2.36E−03)
	HI	Total	2.70	5.94E−01	2.56	5.40E−01	9.17E−01	2.96E−01	(2.68, 2.72)	(5.88E−01, 5.99E−01)
	CR	Co	9.50E−09	4.00E−08	8.16E−09	3.43E−08	5.37E−09	2.25E−08	(9.39E−09, 9.60E−09)	(3.96E−08, 4.04E−08)
		Ni	1.69E−09	7.13E−09	1.62E−09	6.89E−09	7.17E−10	2.97E−09	(1.68E−09, 1.71E−09)	(7.07E−09, 7.19E−09)
		Pb	6.71E−07	4.27E−07	6.35E−07	4.04E−07	2.30E−07	1.95E−07	(6.66E−07, 6.75E−07)	(4.24E−07, 4.31E−07)
		Cr	4.02E−08	5.81E−08	3.54E−08	5.12E−08	2.09E−08	2.92E−08	(3.98E−08, 4.06E−08)	(5.75E−08, 5.87E−08)
		As	9.76E−05	1.41E−04	8.75E−05	1.11E−04	4.94E−05	1.12E−04	(9.67E−05, 9.86E−05)	(1.39E−04, 1.43E−04)
	TCR	Total	9.83E−05	1.41E−04	8.83E−05	1.11E−04	4.94E−05	1.12E−04	(9.74E−05, 9.93E−05)	(1.39E−04, 1.44E−04)

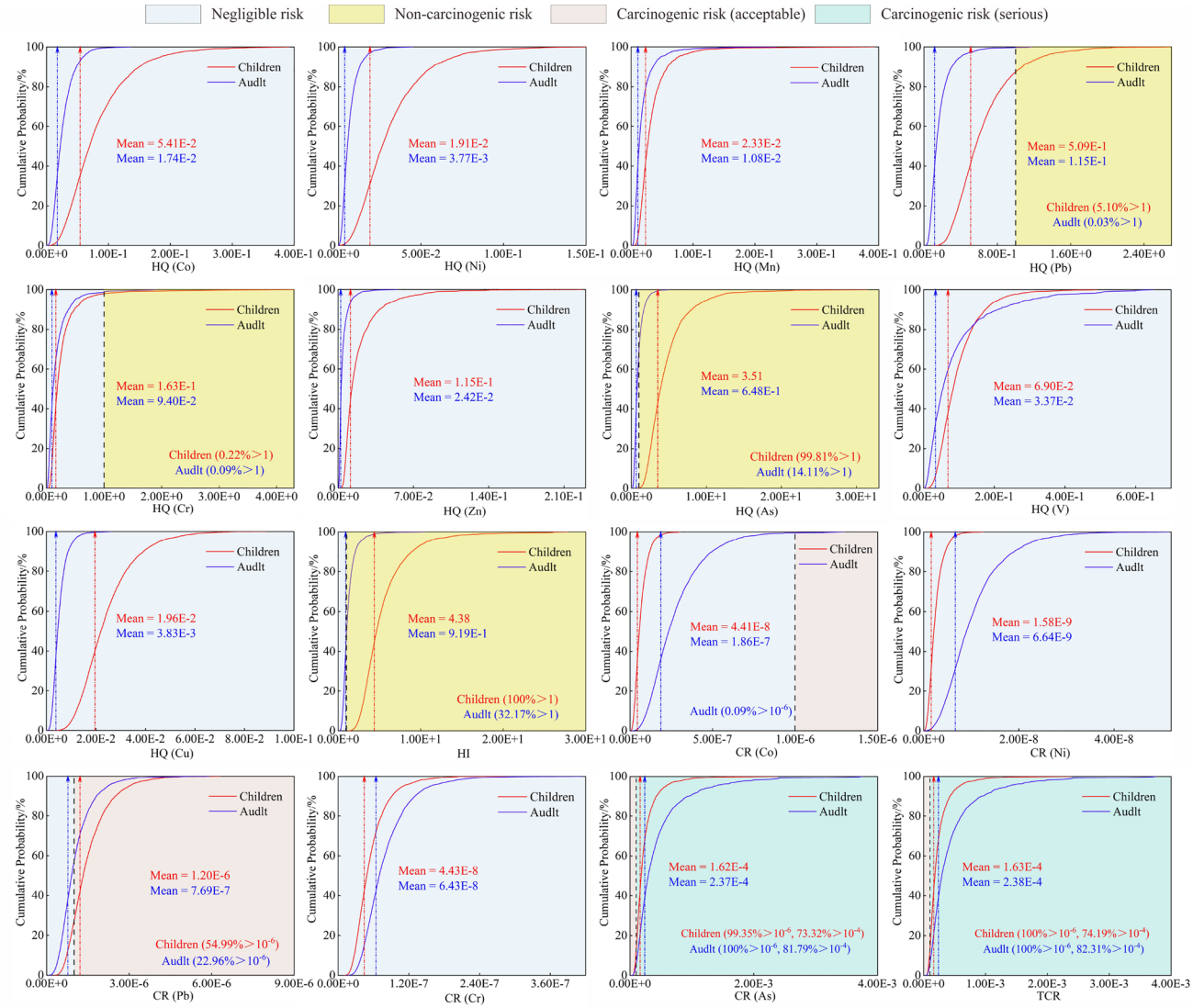

Fig. 5 Cumulative probabilities of the NCR (HQ) and CR (CR) of HMs in QZV (The blue and red dashed lines represent the location of the average risk values for adults and children, respectively)

In LSV, the NCR contributions of the four sources were also distinctly different. Specifically, coal and biomass combustion, vehicle emissions and industrial emissions were the highest. The coal and biomass combustion were major NCR sources at two sites, and the risk share of LSV was lower than that of QZV. Meanwhile, the level of risk caused by vehicle and industrial emissions was greater. The ownership of motor vehicles in 2019 reached 340 million in China and has maintained a high growth rate in recent years (Central People's Government of the People's Republic of China, http://www.gov.cn/). Specifically, vehicle emissions were identified as a major source of $PM_{2.5}$ in several Chinese cities (Wu et al. 2016; Zíková et al. 2016; Chao et al. 2019) and in rural in northern China (Feng et al. 2006), especially in suburban rural areas. The NCR from industrial production activities was also not negligible, and it reached mean values of 6.73E−01 and 1.79E−01 for children and adults, respectively. The coal and biomass combustion for CR were also dominant in all groups at both sites, with approximately 68% (QZV) and 46% (LSV), respectively. Coal and biomass combustion in remote rural areas where coal is the primary energy source contributed more to the CR of residents than in suburban rural areas on the edge of urban centers. The use of coal and the burning of agricultural waste, in addition to raising the population's noncarcinogenic health risks, make people more susceptible to cancer in remote rural areas. As and Pb, which have the highest loads from coal and biomass combustion, should be considered the top pollutants for further risk control.

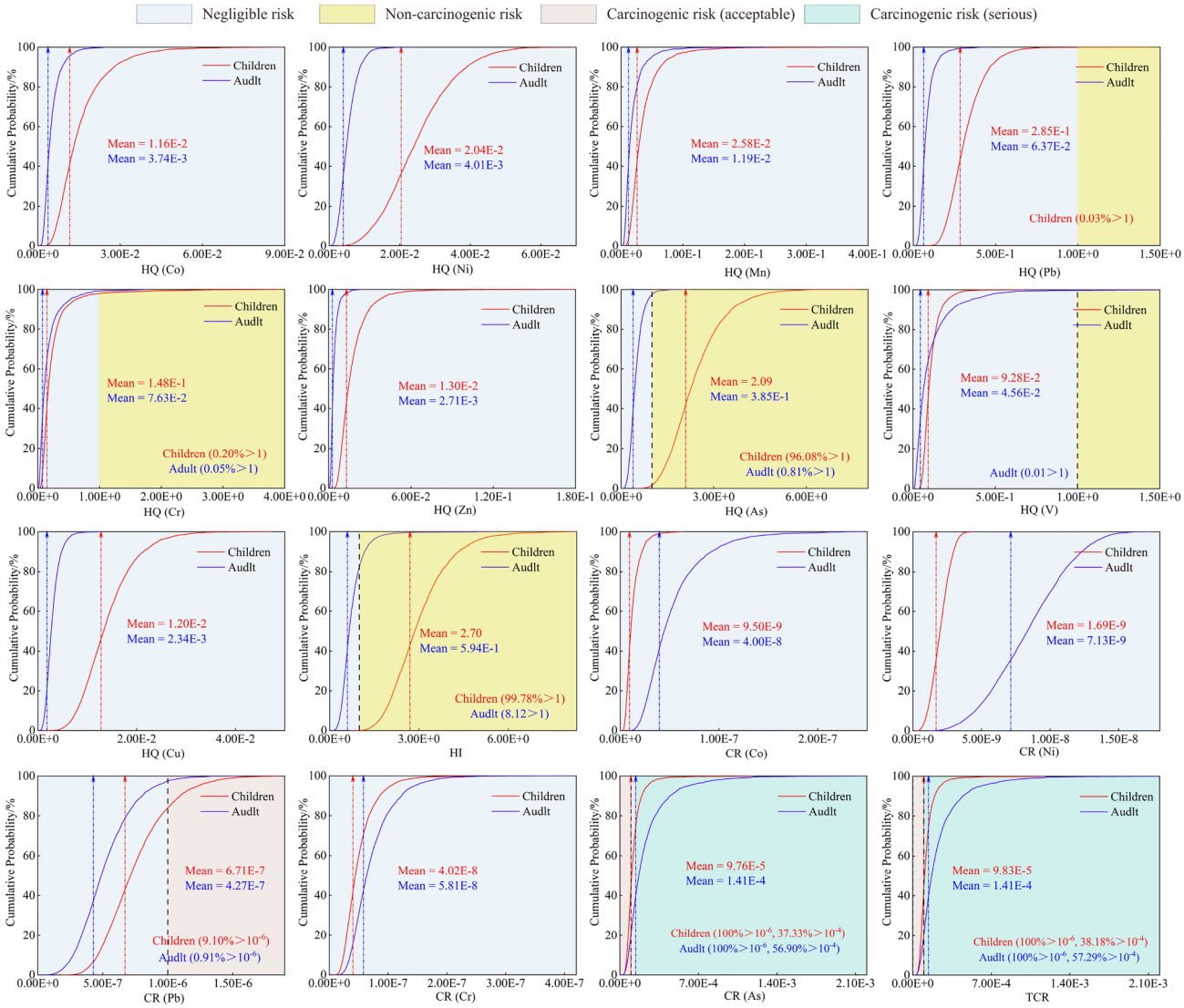

Fig. 6 Cumulative probabilities of the NCR (HQ) and CR (CR) of HMs in LSV (The blue and red dashed lines represent the location of the average risk values for adults and children, respectively)

The NCR of HMs from coal and biomass combustion to the residents was 2.68 times higher in QZV and 2.47 times greater in cancer burden than in LSV, while the health risk from motor vehicle emissions and industrial emissions was lower. This result suggests that the high health risk faced by remote rural populations mainly comes from coal combustion compared with that by rural suburban populations. The spread of electricity and natural gas reduces the health burden on residents from $PM_{2.5}$-bound HMs in rural China, including noncarcinogenic and cancer risks, compared with that of coal. The use of coal and biomass for heating and cooking should be rigorously prohibited in remote rural areas, while motor vehicle exhaust ought to be strictly controlled in suburban rural areas. The health hazards that industrial pollution poses to rural residents must be regarded as an increasing number of highly polluting industries move from the cities to the countryside.

Strengths and Limitations

Differences in health risks among rural populations with dissimilar types of energy use were first proposed, and field observations were implemented in suburban rural and remote rural areas. Probabilistic and source-specific health risk assessments were coupled to reduce the uncertainty introduced by point estimates and provide a scientific basis for risk management directions. However, uncertainties remain in the health risk assessment of this study. Firstly, the CR and NCR exposed to the local population were calculated based only on the sum of the risks of the nine HMs,

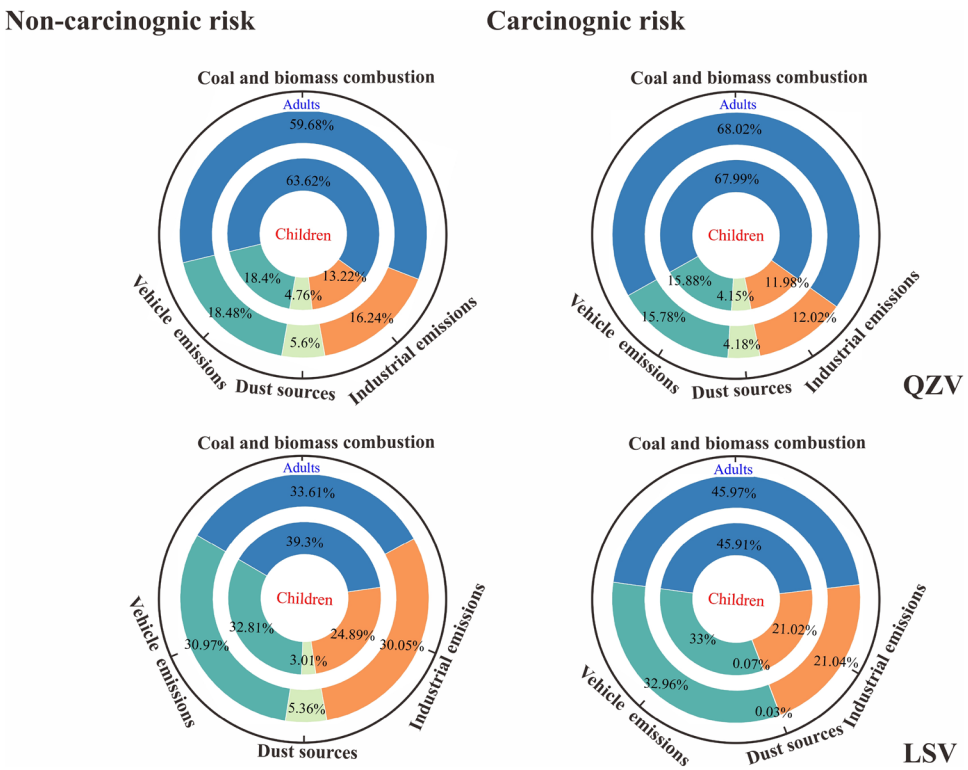

Fig. 7 Relative contribution of each source to the NCR and CR at two sites

and more HM species should be considered, such as Cd and Hg. Secondly, only the total concentrations of HMs were considered in the present study, and health risk assessment based on the total concentration may overestimate the potential health burden relative to that based on bioavailability. The finite number of sampling sites is the limitation, and more research on both rural types is required in the future to complement our perspective.

Conclusion

The likelihood of developing cardiovascular or respiratory diseases, and even premature death due to air pollution exposure, is higher among rural populations than urban ones in China. There is a significant discrepancy between government policies aimed at reducing health risks for rural populations and the actual situation, primarily due to the lack of information about haze pollution in these areas.

Our study quantified the health risks for rural residents using different types of energy during hazy weather. Using a combination of probabilistic and source-specific risk assessment methods in the North China Plain, we found that the average $PM_{2.5}$ mass greatly surpassed the daily guideline recommended by WHO and was higher than in most Chinese cities. Suburban rural areas carried a heavier air pollution burden than remote rural areas. There was considerable variability exists in the probabilistic and source-specific health risks among populations located in rural areas with different energy use types. At the QZV and LSV sites, 100% and 99.78% of children, and 32.17% and 8.12% of adults, respectively, exceeded the acceptable risk threshold of 1 for HI. The TCR values for all populations exceeded 10^{-6}, with higher burdens found in remote rural areas. Children faced higher NCR but lower CR than adults. The NCR of HMs from coal and biomass combustion was 2.68 times higher in QZV and carried 2.47 times more cancer risk than in LSV. However, the health risks from vehicle and industrial emissions were lower. The widespread use of electricity and natural gas decreased the health burden on residents compared with coal. The study recommends coordinated control of both non-carcinogenic and carcinogenic burdens to mitigate the health risks of rural populations exposed to haze.

Coal and biomass combustion in remote rural areas should be considered major control sources due to their significant contributions to pollution. In suburban rural areas, the main focus should be on reducing coal and biomass combustion, vehicle emissions, and industrial emissions. As and Pb, which have the highest loads from coal and biomass combustion, should be prioritized for risk control. During the energy transition, increasing industrial emissions in rural areas pose new challenges for local public health management. Managing $PM_{2.5}$-bound HMs is complex due to the dispersed nature of villages and the high exposure of rural populations in China. There is a need for further extensive

studied on the different types of energy use in rural areas to ensure precise policy direction.

Supplementary Information The online version contains supplementary material available at https://doi.org/10.1007/s12403-023-00590-9.

Author Contributions WW, XZ: investigation, conceptualization, writing, formal analysis, data curation and editing; MW, MW, QH: conceptualization, methodology, supervision, project administration and review; CC, DL: investigation, experimental analysis, data curation, review; QX, CZ: experimental analysis, data curation, investigation and experimental analysis.

Funding This work was supported by the National Natural Science Foundation of China (Grant Number 42177070): Migration processes of pathogenic bacteria at the subsurface media interface in livestock manure return areas and their driving mechanisms.

Data Availability Data available on request from the authors.

Declarations

Conflict of interest The authors have no relevant financial or non-financial interests to disclose.

References

Amato F, Hopke PK (2012) Source apportionment of the ambient $PM_{2.5}$ across St. Louis using constrained positive matrix factorization. Atmos Environ 46:329–337. https://doi.org/10.1016/j.atmosenv.2011.09.062

AMBS (2021) Anyang city statistical yearbook 2021. Anyang Municipal Bureau of Statistics, Anyang

Begum BA, Kim E, Biswas SK, Hopke PK (2004) Investigation of sources of atmospheric aerosol at urban and semi-urban areas in Bangladesh. Atmos Environ 38:3025–3038. https://doi.org/10.1016/j.atmosenv.2004.02.042

Behrooz RD, Kaskaoutis DG, Grivas G, Mihalopoulos N (2021) Human health risk assessment for toxic elements in the extreme ambient dust conditions observed in Sistan, Iran. Chemosphere 262:127835. https://doi.org/10.1016/j.chemosphere.2020.127835

Bell ML, Ebisu K, Leaderer BP, Gent JF, Lee HJ, Koutrakis P, Wang Y, Dominici F, Peng RD (2014) Associations of $PM_{2.5}$ constituents and sources with hospital admissions: analysis of four counties in Connecticut and Massachusetts (USA) for persons >= 65 years of age. Environ Health Perspect 122:138–144. https://doi.org/10.1289/ehp.1306656

Brown SG, Eberly S, Paatero P, Norris GA (2015) Methods for estimating uncertainty in PMF solutions: examples with ambient air and water quality data and guidance on reporting PMF results. Sci Total Environ 518:626–635. https://doi.org/10.1016/j.scitotenv.2015.01.022

Chao S, Liu J, Chen Y, Cao H, Zhang A (2019) Implications of seasonal control of $PM_{2.5}$-bound PAHs: an integrated approach for source apportionment, source region identification and health risk assessment. Environ Pollut 247:685–695. https://doi.org/10.1016/j.envpol.2018.12.074

Chen R, Jia B, Tian Y, Feng Y (2021) Source-specific health risk assessment of $PM_{2.5}$-bound heavy metals based on high time-resolved measurement in a Chinese megacity: insights into seasonal and diurnal variations. Ecotoxicol Environ Saf 216:112167. https://doi.org/10.1016/j.ecoenv.2021.112167

Du W, Li X, Chen Y, Shen G (2018) Household air pollution and personal exposure to air pollutants in rural China—a review. Environ Pollut 237:625–638. https://doi.org/10.1016/j.envpol.2018.02.054

Faraji Ghasemi F, Dobaradaran S, Saeedi R, Nabipour I, Nazmara S, Abadi RV, Arfaeinia H, Ramavandi B, Spitz J, Mohammadi MJ, Keshtkar M (2020) Levels and ecological and health risk assessment of $PM_{2.5}$-bound heavy metals in the northern part of the Persian Gulf. Environ Sci Pollut R 27:5305–5313. https://doi.org/10.1007/s11356-019-07272-7

Feng J, Chan CK, Fang M, Hu M, He L, Tang X (2006) Characteristics of organic matter in $PM_{2.5}$ in Shanghai. Chemosphere 64:1393–1400. https://doi.org/10.1016/j.chemosphere.2005.12.026

Feng J, Yu H, Liu S, Su X, Li Y, Pan Y, Sun J (2017) $PM_{2.5}$ levels, chemical composition and health risk assessment in Xinxiang, a seriously air-polluted city in North China. Environ Geochem Health 39:1071–1083. https://doi.org/10.1007/s10653-016-9874-5

Feng R, Xu H, He K, Wang Z, Han B, Lei R, Ho KF, Niu X, Sun J, Zhang B, Liu P, Shen Z (2021) Effects of domestic solid fuel combustion emissions on the biomarkers of homemakers in rural areas of the Fenwei Plain, China. Ecotoxicol Environ Saf 214:112104. https://doi.org/10.1016/j.ecoenv.2021.112104

Feng R, Xu H, Wang Z, He K, Shen Z, Sun J, Sun N (2022a) Characteristics, sources and health effect of trace components in indoor, outdoor, and personal exposure to $PM_{2.5}$ samples in rural areas of Guanzhong, Shaanxi. Environ Chem 41(7):2334–2346 (**In Chinese**)

Feng X, Shao L, Jones T, Li Y, Cao Y, Zhang M, Ge S, Yang C, Lu J, BeruBe K (2022b) Oxidative potential and water-soluble heavy metals of size-segregated airborne particles in haze and non-haze episodes: impact of the "Comprehensive Action Plan" in China. Sci Total Environ 814(25):152774. https://doi.org/10.1016/j.scitotenv.2021.152774

Guo L, Liu T, He G, Lin H, Hu J, Xiao J, Li X, Zeng W, Zhou Y, Li M, Yu S, Xu Y, Zhang H, Lv Z, Zhang J, Ma W (2021) Short-term mortality risks of daily $PM_{2.5}$-bound metals in urban region of Guangzhou, China, an indication of health risks of $PM_{2.5}$ exposure. Ecotoxicol Environ Saf 228(25):113049. https://doi.org/10.1016/j.ecoenv.2021.113049

Hakanson L (1980) An ecological risk index for aquatic pollution control a sedimentological approach. Water Res 14(8):975–1001. https://doi.org/10.1016/0043-1354(80)90143-8

Han Q, Wang M, Cao J, Gui C, Liu Y, He X, He Y, Liu Y (2020) Health risk assessment and bioaccessibilities of heavy metals for children in soil and dust from urban parks and schools of Jiaozuo, China. Ecotoxicol Environ Saf 191:110157. https://doi.org/10.1016/j.ecoenv.2019.110157

Han Q, Liu Y, Feng X, Mao P, Sun A, Wang M, Wang M (2021a) Pollution effect assessment of industrial activities on potentially toxic metal distribution in windowsill dust and surface soil in central China. Sci Total Environ 759:144023. https://doi.org/10.1016/j.scitotenv.2020.144023

Han X, Li S, Li Z, Pang X, Bao Y, Shi J, Ning P (2021b) Concentrations, source characteristics, and health risk assessment of toxic heavy metals in $PM_{2.5}$ in a Plateau City (Kunming) in Southwest China. Int J Environ Res Public Health 18(21):11004. https://doi.org/10.3390/ijerph182111004

Hassan H, Latif MT, Juneng L, Amil N, Khan MF, Fujii Y, Jamhari AA, Hamid HHA, Banerjee T (2021) Chemical characterization and sources identification of $PM_{2.5}$ in a tropical urban city during non-hazy conditions. Urban Clim 39:100953. https://doi.org/10.1016/j.uclim.2021.100953

Heidari M, Darijani T, Alipour V (2021) Heavy metal pollution of road dust in a city and its highly polluted suburb; quantitative source apportionment and source-specific ecological and health risk assessment. Chemosphere 273:129656. https://doi.org/10.1016/j.chemosphere.2021.129656

Hu R, Wang S, Aunan K, Zhao M, Chen L, Liu Z, Hansen MH (2019) Personal exposure to $PM_{2.5}$ in Chinese rural households in the Yangtze River Delta. Indoor Air 29:403–412. https://doi.org/10.1111/ina.12537

Huang H, Jiang Y, Xu X, Cao X (2018) In vitro bioaccessibility and health risk assessment of heavy metals in atmospheric particulate matters from three different functional areas of Shanghai, China. Sci Total Environ 610:546–554. https://doi.org/10.1016/j.scitotenv.2017.08.074

Huang J, Wu Y, Sun J, Li X, Geng X, Zhao M, Sun T, Fan Z (2021) Health risk assessment of heavy metal(loid)s in park soils of the largest megacity in China by using Monte Carlo simulation coupled with Positive matrix factorization model. J Hazard Mater 415:125629. https://doi.org/10.1016/j.jhazmat.2021.125629

Hus CY, Chi KH, Wu CD, Lin SL, Hsu WC, Tseng CC, Chen MJ, Chen YC (2021) Integrated analysis of source-specific risks for $PM_{2.5}$-bound metals in urban, suburban, rural, and industrial areas. Environ Pollut 275:116652. https://doi.org/10.1016/j.envpol.2021.116652

IARC (2016) Agents classified by the IARC monographs, vol 1–129. International Agency for Research on Cancer, Lyon

Jimenez E, Linares C, Rodriguez LF, Bleda MJ, Diaz J (2009) Short-term impact of particulate matter ($PM_{2.5}$) on daily mortality among the over-75 age group in Madrid (Spain). Sci Total Environ 407:5486–5492. https://doi.org/10.1016/j.scitotenv.2009.06.038

Jin X, Cai X, Yu M, Song Y, Wang X, Kang L, Zhang H (2020) Diagnostic analysis of wintertime $PM_{2.5}$ pollution in the North China Plain: the impacts of regional transport and atmospheric boundary layer variation. Atmos Environ 224:117346. https://doi.org/10.1016/j.atmosenv.2020.117346

Kong SF, Li L, Li XX, Yin Y, Chen K, Liu DT, Yuan L, Zhang YJ, Shan YP, Ji YQ (2015) The impacts of firework burning at the Chinese Spring Festival on air quality: insights of tracers, source evolution and aging processes. Atmos Chem Phys 15:2167–2184. https://doi.org/10.5194/acp-15-2167-2015

Kong L, Tan Q, Feng M, Qu Y, An J, Liu X, Cheng N, Deng Y, Zhai R, Wang Z (2020) Investigating the characteristics and source analyses of $PM_{2.5}$ seasonal variations in Chengdu, Southwest China. Chemosphere 243:125267. https://doi.org/10.1016/j.chemosphere.2019.125267

Lai S, Xie Z, Song T, Tang J, Zhang Y, Mi W, Peng J, Zhao Y, Zou S, Ebinghaus R (2015) Occurrence and dry deposition of organophosphate esters in atmospheric particles over the northern South China Sea. Chemosphere 127:195–200. https://doi.org/10.1016/j.chemosphere.2015.02.015

Li F, Yan J, Wei Y, Zeng J, Wang X, Chen X, Zhang C, Li W, Chen M, Lü G (2021) $PM_{2.5}$-bound heavy metals from the major cities in China: Spatiotemporal distribution, fuzzy exposure assessment and health risk management. J Clean Prod 286:124967. https://doi.org/10.1016/j.jclepro.2020.124967

Liu L (2013) Geographic approaches to resolving environmental problems in search of the path to sustainability: the case of polluting plant relocation in China. Appl Geogr 45:138–146. https://doi.org/10.1016/j.apgeog.2013.08.011

Liu K, Ren J (2020) Seasonal characteristics of $PM_{2.5}$ and its chemical species in the northern rural China. Atmos Pollut Res 11:1891–1901. https://doi.org/10.1016/j.apr.2020.08.005

Liu P, Zhang C, Mu Y, Liu C, Xue C, Ye C, Liu J, Zhang Y, Zhang H (2016) The possible contribution of the periodic emissions from farmers' activities in the North China Plain to atmospheric water-soluble ions in Beijing. Atmos Chem Phys 16:10097–10109. https://doi.org/10.5194/acp-16-10097-2016

Liu J, Chen Y, Chao S, Cao H, Zhang A, Yang Y (2018a) Emission control priority of $PM_{2.5}$-bound heavy metals in different seasons: a comprehensive analysis from health risk perspective. Sci Total Environ 644:20–30. https://doi.org/10.1016/j.scitotenv.2018.06.226

Liu Y, Wang Q, Zhuang W, Yuan Y, Yuan Y, Jiao K, Wang M, Chen Q (2018b) Calculation of Thallium's toxicity coefficient in the evaluation of potential ecological risk index: a case study. Chemosphere 194:562–569. https://doi.org/10.1016/j.chemosphere.2017.12.002

Liu P, Zhang Y, Wu T, Shen Z, Xu H (2019) Acid-extractable heavy metals in $PM_{2.5}$ over Xi'an, China: seasonal distribution and meteorological influence. Environ Sci Pollut R 26:34357–34367. https://doi.org/10.1007/s11356-019-06366-6

Ma W, Tai L, Qiao Z, Zhong L, Wang Z, Fu K, Chen G (2018) Contamination source apportionment and health risk assessment of heavy metals in soil around municipal solid waste incinerator: a case study in North China. Sci Total Environ 631–632:348–357. https://doi.org/10.1016/j.scitotenv.2018.03.011

Massey DD, Kulshrestha A, Taneja A (2013) Particulate matter concentrations and their related metal toxicity in rural residential environment of semi-arid region of India. Atmos Environ 67:278–286. https://doi.org/10.1016/j.atmosenv.2012.11.002

Men C, Liu R, Wang Q, Guo L, Miao Y, Shen Z (2019) Uncertainty analysis in source apportionment of heavy metals in road dust based on positive matrix factorization model and geographic information system. Sci Total Environ 652:27–39. https://doi.org/10.1016/j.scitotenv.2018.10.212

Men C, Liu R, Wang Q, Miao Y, Wang Y, Jiao L, Li L, Cao L, Shen Z, Li Y, Crawford-Brown D (2021) Spatial-temporal characteristics, source-specific variation and uncertainty analysis of health risks associated with heavy metals in road dust in Beijing, China. Environ Pollut 278:116866. https://doi.org/10.1016/j.envpol.2021.116866

Paatero P, Tapper U (1994) Positive matrix factorization: a non-negative factor model with optimal utilization of error estimates of data values. Environmetrics 5:111–126. https://doi.org/10.1002/env.3170050203

Paatero P, Eberly S, Brown SG, Norris GA (2014) Methods for estimating uncertainty in factor analytic solutions. Atmos Meas Tech 7:781–797. https://doi.org/10.5194/amt-7-781-2014

Peng X, Shi G, Liu G, Xu J, Tian Y, Zhang Y, Feng Y, Russell AG (2017) Source apportionment and heavy metal health risk (HMHR) quantification from sources in a southern city in China, using an ME2-HMHR model. Environ Pollut 221:335–342. https://doi.org/10.1016/j.envpol.2016.11.083

Quan J, Tie X, Zhang Q, Liu Q, Li X, Gao Y, Zhao D (2014) Characteristics of heavy aerosol pollution during the 2012–2013 winter in Beijing, China. Atmos Environ 88:83–89. https://doi.org/10.1016/j.atmosenv.2014.01.058

Sah D, Verma PK, Kandikonda MK, Lakhani A (2019) Pollution characteristics, human health risk through multiple exposure pathways, and source apportionment of heavy metals in PM_{10} at Indo-Gangetic site. Urban Clim 27:149–162. https://doi.org/10.1016/j.uclim.2018.11.010

Simoneit BRT, Schauer JJ, Nolte CG, Oros DR, Elias VO, Fraser MP, Rogge WF, Cass GR (1999) Levoglucosan, a tracer for cellulose in biomass burning and atmospheric particles. Atmos Environ 33(2):173–182. https://doi.org/10.1016/S1352-2310(98)00145-9

USEPA (United States Environmental Protection Agency) (2011) Exposure factors handbook, Final edn. U.S. Environment Protection Agency, Washington, DC (EPA/600/R-09/052F). USEPA

Wang S, Li G, Gong Z, Du L, Zhou Q, Meng X, Xie S, Zhou L (2015) Spatial distribution, seasonal variation and regionalization of $PM_{2.5}$ concentrations in China. Sci China Chem 58:1435–1443. https://doi.org/10.1007/s11426-015-5468-9

Wang F, Wang J, Han M, Jia C, Zhou Y (2019a) Heavy metal characteristics and health risk assessment of $PM_{2.5}$ in students' dormitories in a university in Nanjing, China. Build Environ 160:106206. https://doi.org/10.1016/j.buildenv.2019.106206

Wang M, Han Q, Gui C, Cao J, Liu Y, He X, He Y (2019b) Differences in the risk assessment of soil heavy metals between newly built and original parks in Jiaozuo, Henan Province, China. Sci Total Environ 676:1–10. https://doi.org/10.1016/j.scitotenv.2019.03.396

Wang B, Li Y, Tang Z, Cai N, Zhang N, Liu J (2021a) The heavy metals in indoor and outdoor $PM_{2.5}$ from coal-fired and non-coal-fired area. Urban Clim 40:101000. https://doi.org/10.1016/j.uclim.2021.101000

Wang Y, Guo G, Zhang D, Lei M (2021b) An integrated method for source apportionment of heavy metal(loid)s in agricultural soils and model uncertainty analysis. Environ Pollut 276:116666. https://doi.org/10.1016/j.envpol.2021.116666

Wang W, Chen C, Liu D, Wang M, Han Q, Zhang X, Feng X, Sun A, Mao P, Xiong Q, Zhang C (2022) Health risk assessment of $PM_{2.5}$ heavy metals in county units of northern China based on Monte Carlo simulation and APCS-MLR. Sci Total Environ 843:156777. https://doi.org/10.1016/j.scitotenv.2022.156777

Widziewicz K, Loska K (2016) Metal induced inhalation exposure in urban population: a probabilistic approach. Atmos Environ 128:198–207. https://doi.org/10.1016/j.atmosenv.2015.12.061

Wu X, Wu Y, Zhang S, Liu H, Fu L, Hao J (2016) Assessment of vehicle emission programs in China during 1998–2013: achievement, challenges and implications. Environ Pollut 214:556–567. https://doi.org/10.1016/j.envpol.2016.04.042

Wu J, Li J, Teng Y, Chen H, Wang Y (2020) A partition computing-based positive matrix factorization (PC-PMF) approach for the source apportionment of agricultural soil heavy metal contents and associated health risks. J Hazard Mater 388:121766. https://doi.org/10.1016/j.jhazmat.2019.121766

Xie Y, Zhao B, Zhao Y, Luo Q, Wang S, Zhao B, Bai S (2017) Reduction in population exposure to $PM_{2.5}$ and cancer risk due to $PM_{2.5}$-bound PAHs exposure in Beijing, China during the APEC meeting. Environ Pollut 225:338–345. https://doi.org/10.1016/j.envpol.2017.02.059

Xie Y, Liu Z, Wen T, Huang X, Liu J, Tang G, Yang Y, Li X, Shen R, Hu B, Wang Y (2019) Characteristics of chemical composition and seasonal variations of $PM_{2.5}$ in Shijiazhuang, China: impact of primary emissions and secondary formation. Sci Total Environ 677:215–229. https://doi.org/10.1016/j.scitotenv.2019.04.300

Xie Y, Lu H, Yi A, Zhang Z, Zheng N, Fang X, Xiao H (2020) Characterization and source analysis of water-soluble ions in $PM_{2.5}$ at a background site in central China. Atmos Res 239:104881. https://doi.org/10.1016/j.atmosres.2020.104881

Xu H, Cao J, Chow JC, Huang RJ, Shen Z, Chen LW, Ho KF, Watson JG (2016) Inter-annual variability of wintertime $PM_{2.5}$ chemical composition in Xi'an, China: evidences of changing source emissions. Sci Total Environ 545–546:546–555. https://doi.org/10.1016/j.scitotenv.2015.12.070

Xu M, Liu Z, Hu B, Yan G, Zou J, Zhao S, Zhou J, Liu X, Zheng X, Zhang X, Cao J, Guan M, Lv Y, Zhang Y (2022) Chemical characterization and source identification of $PM_{2.5}$ in Luoyang after the clean air actions. J Environ Sci 115:265–276. https://doi.org/10.1016/j.jes.2021.06.021

Yan RH, Peng X, Lin W, He LY, Wei FH, Tang MX, Huang XF (2022) Trends and challenges regarding the source-specific health risk of $PM_{2.5}$-bound metals in a Chinese megacity from 2014 to 2020. Environ Sci Technol. https://doi.org/10.1021/acs.est.1c06948

Zhang J, Zhou X, Wang Z, Yang L, Wang J, Wang W (2018) Trace elements in $PM_{2.5}$ in Shandong Province: source identification and health risk assessment. Sci Total Environ 621:558–577. https://doi.org/10.1016/j.scitotenv.2017.11.292

Zhang X, Eto Y, Aikawa M (2021) Risk assessment and management of $PM_{2.5}$-bound heavy metals in the urban area of Kitakyushu, Japan. Sci Total Environ 795:148748. https://doi.org/10.1016/j.scitotenv.2021.148748

Zhao Z, Lv S, Zhang Y, Zhao Q, Shen L, Xu S, Yu J, Hou J, Jin C (2019) Characteristics and source apportionment of $PM_{2.5}$ in Jiaxing, China. Environ Sci Pollut Res 26:7497. https://doi.org/10.1007/s11356-019-04205-2

Zhao X, Zhao X, Liu P, Ye C, Xue C, Zhang C, Zhang Y, Liu C, Liu J, Chen H, Chen J, Mu Y (2020) Pollution levels, composition characteristics and sources of atmospheric $PM_{2.5}$ in a rural area of the North China Plain during winter. J Environ Sci 95:172–182. https://doi.org/10.1016/j.jes.2020.03.053

Zhao S, Liu S, Hou X, Sun Y, Beazley R (2021) Air pollution and cause-specific mortality: a comparative study of urban and rural areas in China. Chemosphere 262:127884. https://doi.org/10.1016/j.chemosphere.2020.127884

Zhi M, Zhang X, Zhang K, Ussher SJ, Lv W, Li J, Gao J, Luo Y, Meng F (2021) The characteristics of atmospheric particles and metal elements during winter in Beijing: size distribution, source analysis, and environmental risk assessment. Ecotoxicol Environ Saf 211:111937. https://doi.org/10.1016/j.ecoenv.2021.111937

Zíková N, Wang Y, Yang F, Li X, Tian M, Hopke PK (2016) On the source contribution to Beijing $PM_{2.5}$ concentrations. Atmos Environ 134:84–95. https://doi.org/10.1016/j.atmosenv.2016.03.047